



The 16th International Conference on Mobile Systems and Pervasive Computing (MobiSPC)  
August 19-21, 2019, Halifax, Canada

## Real time visualization of asymmetrical sitting posture

Arif Reza Anwary<sup>a\*</sup>, Hamid Bouchachia<sup>a</sup>, Michael Vassallo<sup>b</sup>

<sup>a</sup>Faculty of Science and Technology, Bournemouth University, Bournemouth, BH 5BB, United Kingdom

<sup>b</sup>Royal Bournemouth Hospital, CoPMRE Bournemouth University, United Kingdom

---

### Abstract

Asymmetrical sitting posture (ASP) affects the body mechanics and puts various body segments under strain which may lead to health problems including musculoskeletal pain, low back pain and spinal deformity resulting increased care costs. The tools and methodologies used to assess human posture are often arbitrary and studied by physicians, physiotherapists and researchers in clinical settings. For example, clinical scales such as the Posture Index or Postural Assessment Scale are subjective or semi-subjective, based on visual observation and require clinical expertise to identify asymmetry. More objective gold standard methods such as Motion Capture Systems rely on access to expensive complex equipment based in laboratories. These are not widely available for several reasons including, scarcity of equipment, need for technical staff, time consuming procedures and overall expense. Therefore, there is a need for a low cost, portable automatic posture monitoring system which would help address this challenge. We develop an automatic ASP monitoring system to provide real time visualization and information about sitting posture. We build flexible pressure sensor (FPS) at six different locations on a chair to collect pressure information using piezoresistive conductive film. The collected data from FPSs are then transferred to a smartphone application using Bluetooth. We develop a dedicated Android App to collect FPSs reading and provide real time visualizations of information. The results show that FPS can be used for objective monitoring of sitting posture. It can also be utilized to provide useful information about patients with pelvic asymmetry in rehabilitation medicine. Our system would significantly simplify the sitting posture monitoring protocols and open possibilities for office, school and home based assessment and support for posture improvement. Furthermore, results from this study will be used to develop a new quantitative posture measurement tool for clinical use.

© 2019 The Authors. Published by Elsevier B.V.

This is an open access article under the CC BY-NC-ND license (<http://creativecommons.org/licenses/by-nc-nd/4.0/>)

Peer-review under responsibility of the Conference Program Chairs.

*Keywords:* Asymmetry Posture Monitoring; Pressure Sensors; Piezoresistive Film; Mobile Healthcare; Smart Sitting

---

\* Corresponding author. Tel.: +44 (0) 1202 61217.

E-mail address: [manwary@bournemouth.ac.uk](mailto:manwary@bournemouth.ac.uk)

## 1. Introduction

Sitting with an upright (a straight back and shoulder), symmetrical (same weight transferred from both sides to supporting area by sit bones) and stable posture (remove weight from the feet) are essential for avoiding ergonomic problems [1]. There are common asymmetric sitting positions such as sitting slumped to one side with the spine bent; keeping knees, ankles, or arms crossed; chin resting on a hand; thick object/s (wallet, cell phones, and paper documents) in the rare pocket; and lying prone on a desk etc. These asymmetric sitting postures are associated with respect to the vertical axis, in the frontal or sagittal planes alignment known as pelvic asymmetry [2].

Asymmetrical sitting promotes non-neutral spine postures and reduces seat pan contact area [3] therefore not recommended, even for short duration exposures. It alters the body mechanics, puts various body segments under strain, hence, contributing to musculoskeletal pain [4]. Asymmetric postures are among the leading causes (80–90%) for low back pain [5]. Crossed legs sitting leads to asymmetric usage of abdominal internal and external oblique muscles that may cause spinal imbalance [6]. Again, lumbar vertebrae are weak for flexing or twisting though they are well tolerable with pressing, crossed legs sitting may also result in back pain [7]. More than 80% of student sit resting their chin on to one hand during their study behind a desk [8]. Such posture with long spending time may cause permanent disparity of shoulder height, placement of eyes, and position of hips [9]. In addition, such posture inevitably leads to instability of musculoskeletal non-equilibrium and spinal [10]. Asymmetric sitting such as sitting with the chin resting on a hand or with crossed legs, which arise from poor habits, may affect spinal balance and may lead to permanent spinal deformity such as kyphosis, scoliosis and lordosis [11]. The tools and methodologies used to assess posture are often arbitrary and often studied in artificial controlled conditions. Posture asymmetries are generally assessed and reported by physicians, physiotherapists and researchers in clinical settings or in laboratories [12]. The scales such as posture index [13] and Postural Assessment Scale [14] used to analyse posture parameters in clinical assessment are mainly subjective or semi-subjective, mostly based on visual observation and require clinical expertise. More objective gold standard methods such as Motion Capture System [15] to analyse posture rely on accessing to expensive complex equipment based in gait laboratories and hence not widely available for several reasons including requirement for expensive equipment, need for technical clinical staff, need for patients to attend in person, complicated time consuming procedures and overall expense. Therefore, it is now a global imperative to address this challenge.

One element that may contribute to avoid asymmetrical sitting is to design and develop automatic real-time monitoring of sitting posture and provide timely interventions through mobile phone or computer. In this study, we design, develop and implement a wearable tool to monitor sitting and visualize asymmetry of sitting posture based on pressure distribution six different locations on a chair. The main contributions of this study are:

- 1) Design and implementation of a new hardware system (focusing on manufacturability, customisation and adaptability) to
  - a) sense pressure using piezoresistive polymer film embedded on a chair. The films are arranged considering on human sitting biomechanics; b) reduce noise using Kalman filter; c) transfer data using Bluetooth wireless connection; and d) manage power supply using wireless charging facility
- 2) Design and development of a dedicated and sophisticated smartphone application that results an extensive testing and improvement scope to ensure accurate and robust results for real time use that
  - a) proposes a simple asymmetry sitting posture visualization technique using dial displays; b) estimates duration of active, static and asymmetrical sitting; and d) proposes scores of the daily asymmetrical sitting duration

## 2. System design

Developing of an automatic real time asymmetric sitting posture monitoring system requires incorporation of hardware and software components. Software components are Arduino programming and development of an Android App. Therefore, the proposed system has main two parts hardware and Android App. The overview of the system is shown in Figure 1.

The hardware part consists of five components. It starts with developing the FPS where we design and fabricate the sensor system. The raw data collected from the FPSs passes through Kalman filter to reduce noise. The next

component is wireless data transfer to a smart phone where our developed Android app receives FPS reading using Bluetooth technology. Inductive wireless technology is used to recharge. Considering these components, the circuit is designed, simulated and implemented. The Android App part has also five components. It starts with receiving the FPS data. The data may require a level of calibration timely to get accurate output. The data is then analyzed to prepare for visualization. A scoring is estimated based on the asymmetrical sitting duration. The last component is to store data for further analysis. Figure 1 depicts the architecture of the system.

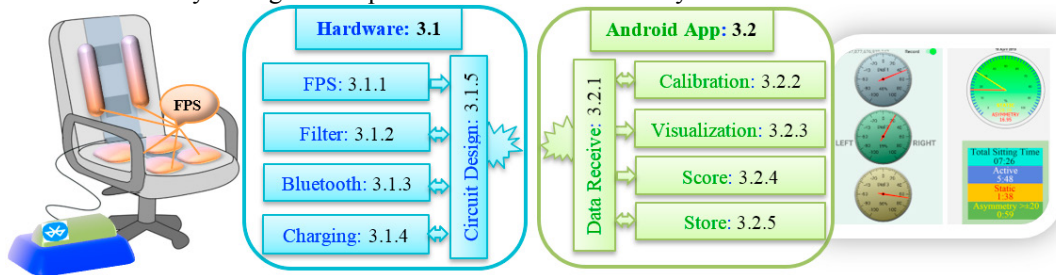


Fig. 1. Architecture of the proposed asymmetric sitting posture monitoring system

2.1. Hardware system: design, architecture and methodology

2.1.1. Flexible pressure sensing system

Piezoresistive materials have the characteristics to change in electrical resistivity when the material is deformed [16]. Therefore, piezoresistive conductive films are suitable to use as pressure sensors due to their simple structure in different applications. Velostat is an antistatic piezoresistive conductive film with the properties: volume resistivity  $< 500 \text{ ohm-cm}$ , typical thickness  $104 \text{ }\mu\text{m}$ , flexural modulus  $40,000\text{-}50,000 \text{ psi}$ , and tensile strength of  $1,700\text{-}2,000 \text{ psi}$  [17]. In this study, a multi-layered architecture of flexible pressure sensor (FPS) is build using Velostat, conductive copper and plastic film. The main components associated with the FPS are depicted in Figure 2.

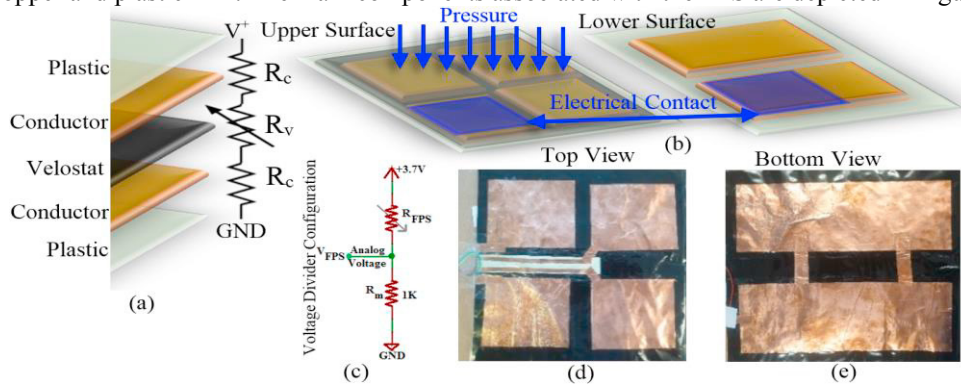


Fig. 2. Flexible pressure sensor; (a) Architecture, components and current flow ( $R_c$  and  $R_v$  are the corresponding resistances of the copper and Velostat); (b) Current through loaded contact area from upper surface to lower surface; (c) Analog output ( $V_{FPS}$ ) reading using voltage divider configuration; (d) Top view of the fabricated sensor; and (e) Bottom view of the fabricated sensor

Figure 2(a) shows the architecture of the FPS which is made with a thin layer of Velostat composite sandwiched between two layers of conductive material (copper). The conductive materials are then covered with two layers of thin adhesive plastic films to protect from dust, wet and displacement of the structure etc. The sensor is modelled with electrical components where the conductive resistance is  $R_c$  and the Velostat resistance is  $R_v$ . During a sitting posture, a compressive pressure is applied to the upper surface of the FPS and the lower surface is solid flat, therefore the pressure results the decrease in resistance because of dropping resistance of the Velostat and also because to a slight dropping in the contact resistance between the conductive material and the Velostat that is depicted in Figure 2(b). As we know that applying a pressure results a decrease in distance between filler particles inside the piezoresistive conductive film which increases in the number of conductive paths, that results in a decrease in resistance of the piezoresistive conductive film [18]. Therefore, the Velostat resistance  $R_v$  changes due to

sitting pressure onto the upper surface. In order to obtain an accurate reading of the FPS output  $S_i$ , the contact resistance  $R_c$  between conductive material and the Velostat is taken into account. The effective area of the electrical contact between the upper surface and lower surface (Figure 2(b) blue marked) is a fraction of the apparent area of contact. In a microscopic scale, the electrical effective contact between two adjacent members is only a small fraction [19] that is obvious the roughness of the surfaces. Since the copper and Velostat are sandwiched among two plastic films, there is no film resistance caused by thin oxide layers on the contact surfaces. Therefore, the total resistance of the FPS can be described by  $R_{FPS} = 2R_c + R_v$  where  $R_{FPS}$  is the total resistance of the FPS and  $R_c$  is the contact resistance between each copper and Velostat. The resistance of the Velostat is  $R_v$ . To convert the pressure to voltage, we design a voltage divider configuration to measure the resistance change of the FPS and a voltage follower as a general setting for impedance matching shown in Figure 2(c). The  $R_m$  is the resistance of the voltage divider. The output of the FPS is then expressed by  $V_{FPS} = (R_{FPS} * V+) / (R_m + R_{FPS})$  where the output voltage of FPS is  $V_{FPS}$  and the supply voltage  $V+$  is 5V. To estimate the appropriate values of  $R_m$  we investigate the output  $V_{FPS}$  changes due to the weights applied to the FPS in increments of load (kg) on different values of  $R_m$ . Based on the applied force vs resistance [20] of the  $R_m$  and our experiment, we set the value of  $R_m$  as 1K  $\Omega$ . The supply voltage of this circuit is set at +5V. The placing of FPS to the locations on a chair is important to get accurate results for monitoring ASP. As FPS is designed in primarily for the application of monitoring ASP in this research and hence it is based on analysis of human upper body dimensions [21]. During a sitting position, human shoulder width range is 375 mm to 505 mm, shoulder height is 505 mm to 646 mm and hip width range is 310 mm to 405 mm [22]. To place the FPS, the seat is primarily divided into four regions: 1) Right thigh region, 2) Left thigh region, 3) Right buttock region and 4) Left buttock region. These regions allow for the description of the pressure distribution of each region. Therefore, each FPS is placed and aligned with the center of each four regions. The top view of the FPS on a chair is shown in Figure 2 (d) and bottom view in Figure 2 (e). The shoulder area of the chair is divided in to two regions in the vertical axis. Two long FPS are placed at the center of these locations. The sitting pressure distribution from a total of six locations (four on seat area and two on shoulder area) are collected with a sampling rate at 10Hz (see Figure 3(a)).

### 2.1.2. Raw data filter

The raw data from these six FPS may contain some noise such mechanical, stretching, constant bias, flicker noise, temperature effects and calibration errors [23]. The readings from the FPS consists of noisy spikes in the plotted graph which is required to remove before using the data for analysis. One way of reducing noise is to apply advanced optimal recursive filter techniques such as Kalman filter [24]. It [25] is a filtering algorithm which can remove noise from a signal while retaining the useful information. It uses a feedback control mechanism in order to estimate a process. Noisy measurements are taken as feedback and using them, the process is estimated. The recursive approach for minimizing errors ensures that estimated state from previous step and current measurement are used to estimate the current state, therefore no history of previous measurements is required. Therefore, Kalman filter is used to reduce noise and obtain distortion-free stabilize reading from FPSs. The readings from FPSs is then wirelessly transmitted to smartphone using Bluetooth for analysis.

### 2.1.3. FPS data transfer using wireless communication

Different types of wireless technologies are currently available for data transmission such as Bluetooth [26], Global system for mobile [27], ZigBee [28], General packet radio service [29], Z-Wave [30], Infrared [31] and Wi-Fi [32]. Bluetooth network has ability to transmit data serially up to 3 Mbps within a physical range of 10 -100 meter depending on the type of Bluetooth device. Bluetooth can connect with smartphone using serial communication. The reading from six FPS are transferred to our developed Smartphone application using Bluetooth technology. It is affordable and easy to interface with circuit. A power supply is essential part to keep the system running smoothly and managing the power is important to run the system for long time.

### 2.1.4. Power supply management

Lowering the duty cycle between the Bluetooth and smartphone can be used to extend the battery life. A two-way push switch is used to control the circuit power. The first push is "OFF" state and the microcontroller stops reading FPS, Bluetooth transmitter stops data transfer and the circuit becomes inactive. The second push on the switch is

“ON” state enable the circuit. To recharge the battery, a wireless inductive power transfer [33] technology is used. It is comprised of two coils: primary coil and secondary coil. A primary coil is an energy transmitter which generates a varying magnetic field. A secondary coil is an energy receiver. The primary coil places across the secondary coil to receive energy within the field. The secondary coil is tuned at the operating frequency to enhance charging efficiency. Considering the above description of the concepts a circuit is designed and described in the next section.

### 2.1.5. Circuit design

An Arduino Nano in the asymmetrical sitting monitoring system acts as a base station. Arduino integrated development environment (IDE) is a cross-platform application programming software provides monitoring facility of the outputs coming from sensor nodes on serial monitor. As Arduino Nano is low cost, low power standard and most flexible system employ with wireless monitoring, it is widely used as an open source hardware and software platform for development. In this research, the Arduino Nano which is a 30pin board having ATmega328 as a microcontroller embedded into it. The ATmega328 has 32 KB, (also with 2KB used for bootloader) of flash-memory and 2 KB of SRAM and 1 KB of EEPROM. It has 14 digital input/output, 8 analog reference pins and has a clock frequency of 16MHz. It consists of analog voltage interface pins from A0 to A7. Analog output from sensors are usually interfaced with the Arduino using these analog pins. There is an analog reference pin (AREF) to compare the output from the sensor node to the voltage with the AREF. The six FPSs (see Figure 3(a)) are connected with six voltage divider configurations (see Figure 2(c)) to obtain  $V_{FPS1 \text{ to } 6}$ . The outputs of these voltage divider  $V_{FPS1 \text{ to } 6}$  are connected with Arduino analog voltage pins A0 to A5. The data gathered by A0 to A5 nodes are being passing on to the base station through serial communication. The serial communication pins used both to receive (*Rx*) and transmit (*Tx*) serial data. The *Rx* and *Tx* in the Arduino Nano are Pin no. 0 and 1. These two pins are connected to the Bluetooth HC-06 module. HC-06 module is an easy to use Bluetooth Serial Port Protocol (*Rx-Tx*), designed for transparent wireless serial connection setup. Serial port Bluetooth module is fully compatible of Bluetooth V4.0+EDR (Enhanced Data Rate) up to 3Mbps Modulation with complete 2.4GHz radio transceiver and baseband. The Bluetooth module HC-06 is a slave device that can operate at a supply power of 3.3 to 6 volts. Therefore, HC-06 is used for wireless communication between the Arduino Nano and Smartphone.

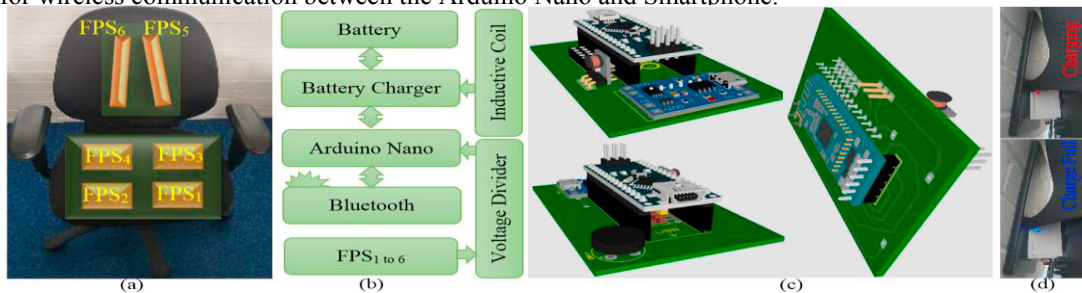


Fig. 3. Overview of the system; (a) FPS arrangement on a chair; (b) Circuit block diagram; (c) 3D view of the simulated circuit (d)

#### Implemented circuit and wireless inductive charging

The operating voltage of the Arduino Nano is 5V. As the battery power supply is 3.7V and Arduino Nano operates on 5V, a DC-DC boost converter is designed to provide regulated 5V supply for the Arduino Nano. TP4056 charging module has been used to charge a BRC 18650 Li-ion 3.7V 4000mAh capacity battery. Qi wireless charging coil is connected with TP4056 to charge the battery. It has Ti clip coil patch that can charge up to 1000 mAh, 5V which meets faster charge and higher conversion rate. The block diagram of the circuit design is shown in Figure 3(b). The circuit is simulated using Proteus ISIS Professional (simulation software of the Labcenter Electronics Corporation [34]) and the 3D view of the device is depicted in Figure 3(c). The circuit schematic, PCB and 3DS files are provided in the supporting document. The implemented circuit with the wireless charging system is shown in Figure 3(d). The charging system has indicators to show charging by red LED and fully charged by blue LED.

## 2.2. Design and development of Android App

Smartphone and apps are an important tool for accessing information. Smartphones have built-in Bluetooth technology to receive or transmit wireless data. As per the architecture of Android, there are four types of app components: *activities*, *service*, *content providers* and *broadcast receivers* [35]. A user interface with the app is *activities*. *Service* provides the background processing. To store and share data, *content providers* use a relational database. *Broadcast receivers* can receive broadcast messages from other applications. The primary method for both within and between applications for inter-component communication is via intents messaging object. In this research, we focus on communication between activity components to send an intent and manifest file specifies filters that are used by the system to determine if the app is eligible to receive a particular data format intent using Android defined rules for matching filters to content various intent fields. The app is designed considering a) Requirement: Requirement analysis is conducted through the literature review, discussion with the expert and users, b) Market availability: The market available mobile software development platforms are reviewed. Mobile platforms and supporting devices are selected considering hardware performance, battery life, ruggedness, required peripherals, device coverage, device support and performance, c) Initial design: Activity classes are reviewed including SplashActivity, MenuActivity, PlayActivity and HelpActivity etc. A very basic design is implemented using Android Studio 3.4, d) Testing and debugging: The app is tested and users' feedbacks are recorded. All issues are addressed, the app is improvement and documented, and e) Multi-sensor synchronous data collection: The app is designed to collect up multiple sensors data synchronous through Bluetooth.

### 2.2.1. Data receive

An Android app is developed to collect and display real time asymmetric sitting posture information. The Samsung S9 smartphone is used to connect with Bluetooth and collect FPSs data. The data receiving format is date (*dd/mm/yyyy*), time (*HH:MM:SS.ss*), system clock (Millisecond), and FPS(*FPS<sub>1</sub>*, *FPS<sub>2</sub>*, *FPS<sub>3</sub>*, *FPS<sub>4</sub>*, *FPS<sub>5</sub>*, *FPS<sub>6</sub>*). Initially a "SCAN" button on the app is pressed to list available all Bluetooth devices in the coverage area. From the list, our Bluetooth device is selected and the corresponding device then automatically connects. The data comes to a buffer and used for analysis.

### 2.2.2. Calibration

The FPS based on piezoresistive conductive film is very sensitive to pressure, force and stretch. At the initial stage of the FPS shows some values due to internal resistance or mechanical structure. Therefore, the output of the FPS needs to be calibrated before performing analysis. Before sitting on to the chair, the initial values of the individual FPS are recorded as initial threshold values. User is then asked to sit on to the chair and perform movements to different directions. The maximum values due to sitting pressure for individual FPS are also recorded as maximum threshold values. The initial threshold values are then subtracted to set each FPS at zero and estimate maximum threshold values and stored in log file. This calibration procedure is followed once in a week and it varies from individuals. Every time the app runs, it restores the values from log file and updates to new parameters after each calibration.

### 2.2.3. Visualization

To visualize the ASP, the reading from FPS<sub>1</sub> to FPS<sub>6</sub> is used. Initially the maximum (*max*) and minimum (*min*) threshold values are restored from the log file mentioned in Section 3.2.2 from individual FPS. We then draw a circle from  $\theta=0$  to  $2\pi$  of duration of 0.01 using  $x = \sin(\theta)$ ,  $y = \cos(\theta)$ . We define the interval  $\alpha=50$  and the value of each step increment ( $\delta$ ) is computed by  $\delta = (\max - \min) / \alpha$ . The interval angle  $\omega$  is estimated using  $\omega = \lambda * \pi / \alpha$  with  $\lambda=1$ . The scale is represented from 0 to  $\alpha$  using  $\gamma = -\lambda * \pi / i * n + \lambda * \pi$ , for  $n=0$  to  $\alpha$ . The small scale line is then drawn using  $x = \sin(\gamma)$ ,  $y = \cos(\gamma)$ . The minimum and maximum values of the scale are mapped between -100 to +100. The indicator line ( $\beta$ ) is then set with the instantaneous difference between left and right value of the feature ( $\eta$ ) using  $\beta = -\omega * (\eta - \min) / \delta + \lambda * \pi$ . The indicator line is drawn from 0 to  $\beta$ . The asymmetry between right and left thigh is represented by the difference between FPS<sub>5</sub> and FPS<sub>6</sub> (see Figure3 (a)), between right and left buttock region is represented by the difference between FPS<sub>3</sub> and FPS<sub>4</sub>, and between right and left shoulder region is represented by the difference between FPS<sub>1</sub> and FPS<sub>2</sub>. The overview of the visualization of



ASP is shown in Figure 4. Figure 4(a) shows a posture with asymmetrical sitting in cross-leg position and Figure 4(b) demonstrates asymmetrical measurements in a dial fashion. During a sitting posture, the pressure distribution of both right and left side should theoretically give identical results and therefore perfect asymmetry should give dial indicator readings of zero. The first dial (Dial 1), second dial (Dial 2), and third dial (Dial 3) are displaying asymmetry for thigh, buttock, and shoulder regions. It is noted that there is a difference in the level of asymmetry. For example, red indicator in Dial 1 shows a reading of around +44, it means that the pressure distribution of the right shoulder region is higher than the left. A negative value indicates the pressure of the left region is higher than the right region. A high reading indicates higher asymmetry and a low reading indicates good sitting posture. The app records daily reading and estimates duration of total sitting, active, static and asymmetry sittings.

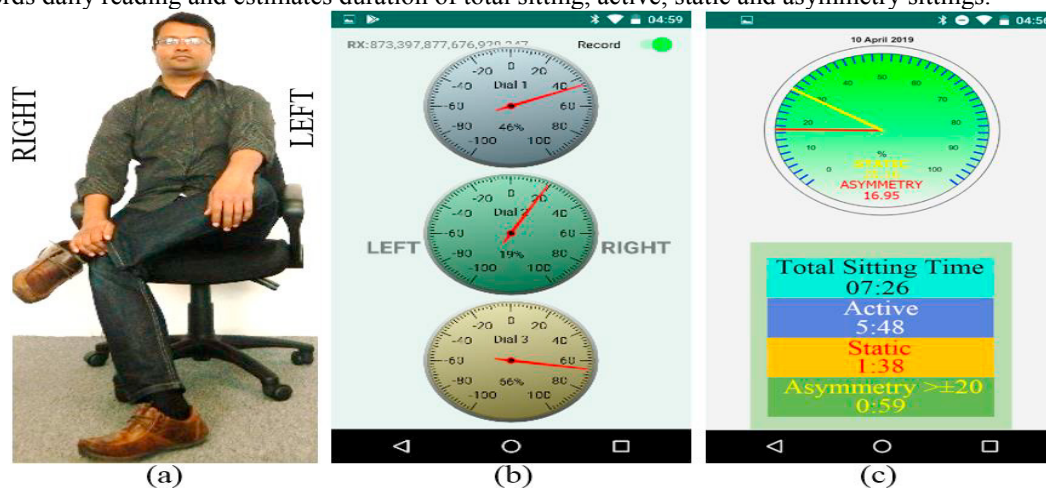


Fig. 4. (a) Sample representation of asymmetrical sitting posture; (b) Dial based asymmetrical sitting posture visualization; (c) Sitting score and summary for a day

#### 2.2.4. Score

The duration of everyday sitting time is estimated. The duration of the active sitting is estimated when there is non-zero reading from all six FPS. The duration of static sitting is estimated when the dials reading values lie less than  $\pm 5$ . The duration of the asymmetric sitting is estimated when any dial shows more than  $\pm 20$  for more than 5 minutes. A static sitting score is estimated using percentage by  $STATIC = (\text{duration of static sitting} / \text{duration of active sitting}) * 100$ . An asymmetric sitting score is estimated using percentage by  $ASYMMETRY = (\text{duration of asymmetric sitting} / \text{duration of active sitting}) * 100$ . The details of estimations and scores are presented in Figure 4(c). A low score indicates good sitting posture.

#### 2.2.5. Data store

The app has the facility to store data on an internal/external location as a csv file. There is a switch “Record” at the top right side of the app, pressing it starts data storing. The switch is pressed again to stop; the collected data is stored as a csv file. In future, data from patients with posture disorders will be stored in cloud platform to bring out new information using artificial intelligence and allow accessible to stake holders including patients’, general practitioners, therapists, social carers and hospital specialists to facilitate the interaction between the relevant members of the group who can make treatment recommendations and follow progress remotely.

### 3. Conclusion

In this research, we designed, developed and implemented a low cost new hardware and Android App to monitor and improve sitting posture. The paper describes a healthy sitting monitoring system. While systems to monitor posture have been developed [36] our system differs by integrating posture visualization in real time with post data-collection analysis. As part of this research, we build a flexible pressure sensor considering the sitting presser sensing system compatible with human biomechanics for use embedded in complex interfaces, such as seat cover

and chair. Our flexible pressure sensors use a novel multi-layering method which is proposed as a full solution for manufacturing and real world use. The flexible nature of the sensors allows us to design for anthropomorphic parameters of varying human back sizes and variations in chair shapes. Bluetooth is used to transfer sensor data to a smart phone application. The inducting charging system helps to maximize the battery runtime and auto cut protects the battery from over charge. Our designed and developed Android App provides graphical dial based visualization of the real time sitting posture information and stores data to provide daily scores. This offers an easy, user friendly private and secure way to visualize and monitor sitting posture which can be used for monitoring and rehabilitation purpose of diseases associated with sitting posture in different clinical setting, work place, school and patient's home. This study adds to current literature by demonstrating a new visual method of demonstrating real time asymmetry sitting posture that increases the reliability and validity of monitoring posture abnormalities.

## References

- [1] N. Krause, R. Rugulies, D. R. Ragland, and S. L. Syme, "Physical workload, ergonomic problems, and incidence of low back injury: A 7.5 - year prospective study of San Francisco transit operators," *American journal of industrial medicine*, vol. 46, pp. 570-585, 2004.
- [2] J. Dubouset, "Pelvic obliquity: a review," *Orthopedics*, vol. 14, pp. 479-481, 1991.
- [3] D. Viggiani, M. Noguchi, K. M. Gruevski, D. De Carvalho, and J. P. Callaghan, "The Effect of Wallet Thickness on Spine Posture, Seat Interface Pressure, and Perceived Discomfort During Sitting," *IIE Transactions on Occupational Ergonomics and Human Factors*, vol. 2, pp. 83-93, 2014.
- [4] E. Al-Eisa, D. Egan, and A. Fenety, "Association between lateral pelvic tilt and asymmetry in sitting pressure distribution," *Journal of Manual & Manipulative Therapy*, vol. 12, pp. 133-142, 2004.
- [5] E. Al-Eisa, D. Egan, K. Deluzio, and R. Wassersug, "Effects of pelvic asymmetry and low back pain on trunk kinematics during sitting: a comparison with standing," *Spine*, vol. 31, pp. E135-E143, 2006.
- [6] G. Harris, R. Pudlowski, E. Abraham, and E. Millar, "Thoracic suspension: quantitative effects upon seating pressure and posture," *Spinal Cord*, vol. 25, p. 446, 1987.
- [7] S.-y. Kang, S.-H. Kim, S.-J. Ahn, Y.-H. Kim, and H.-S. Jeon, "A comparison of pelvic, spine angle and buttock pressure in various cross-legged sitting postures," *Physical Therapy Korea*, vol. 19, pp. 1-9, 2012.
- [8] K. M. Alexander and T. L. Kinney LaPier, "Differences in static balance and weight distribution between normal subjects and subjects with chronic unilateral low back pain," *Journal of orthopaedic & sports physical therapy*, vol. 28, pp. 378-383, 1998.
- [9] C. Phimphasak, M. Swangnetr, R. Puntumetakul, U. Chatchawan, and R. Boucaut, "Effects of seated lumbar extension postures on spinal height and lumbar range of motion during prolonged sitting," *Ergonomics*, vol. 59, pp. 112-120, 2016.
- [10] J. B. Myers and S. M. Lephart, "The role of the sensorimotor system in the athletic shoulder," *Journal of athletic training*, vol. 35, p. 351, 2000.
- [11] M.-J. Kim, C.-G. Son, D.-S. Heo, and K.-E. Hong, "Analysis of clinical tendency of spinal disorder in primary, middle and high school students in Korea," *THE ACUPUNCTURE*, vol. 27, 2010.
- [12] M. Mock and K. Sweeting, "Gait and posture-assessment in general practice," *Australian family physician*, vol. 36, p. 398, 2007.
- [13] G. Fröhner, "Objectification of posture and trunk flexibility in children and adolescents," *Haltung Bewegung*, vol. 2, pp. 5-13, 1998.
- [14] C.-W. Chien, J.-H. Lin, C.-H. Wang, I.-P. Hsueh, C.-F. Sheu, and C.-L. Hsieh, "Developing a short form of the postural assessment scale for people with stroke," *Neurorehabilitation and neural repair*, vol. 21, pp. 81-90, 2007.
- [15] J. L. Garrido-Castro, R. Medina-Carnicer, R. Schiottis, A. M. Galisteo, E. Collantes-Estevez, and C. Gonzalez-Navas, "Assessment of spinal mobility in ankylosing spondylitis using a video-based motion capture system," *Manual therapy*, vol. 17, pp. 422-426, 2012.
- [16] R. W. Christiansen and W. M. Westberg, "Conductive elastomeric fabric and body strap," ed: Google Patents, 1983.
- [17] L. Bolton, B. Folen, B. Means, and S. Petrucelli, "Direct-current bactericidal effect on intact skin," *Antimicrobial agents and chemotherapy*, vol. 18, pp. 137-141, 1980.
- [18] M. Kalantari, J. Dargahi, J. Kövecses, M. G. Mardasi, and S. Nouri, "A new approach for modeling piezoresistive force sensors based on semiconductive polymer composites," *IEEE/ASME Transactions on Mechatronics*, vol. 17, pp. 572-581, 2012.
- [19] R. Holm, *Electric contacts: theory and application*: Springer Science & Business Media, 2013.
- [20] Y. Zhang, J. Ye, Z. Lin, S. Huang, H. Wang, and H. Wu, "A Piezoresistive Tactile Sensor for a Large Area Employing Neural Network," *Sensors*, vol. 19, p. 27, 2019.
- [21] H. Dreyfuss, H. D. Associates, and A. R. Tilley, *The measure of man and woman: human factors in design*: Whitney Library of Design, 1993.
- [22] W. G. Allread and E. W. Israelski, "Anthropometry and biomechanics," in *Handbook of Human Factors in Medical Device Design*, ed: CRC Press, 2010, pp. 106-160.
- [23] J. Heikenfeld, A. Jajack, J. Rogers, P. Gutruf, L. Tian, T. Pan, et al., "Wearable sensors: modalities, challenges, and prospects," *Lab on a Chip*, vol. 18, pp. 217-248, 2018.
- [24] X. Yun and E. R. Bachmann, "Design, implementation, and experimental results of a quaternion-based Kalman filter for human body motion tracking," *IEEE transactions on Robotics*, vol. 22, pp. 1216-1227, 2006.
- [25] R. E. Kalman, "A new approach to linear filtering and prediction problems," *Journal of basic Engineering*, vol. 82, pp. 35-45, 1960.
- [26] J. C. Haartsen, "Bluetooth radio system," *Wiley Encyclopedia of Telecommunications*, 2003.
- [27] M. Mouly, M.-B. Pautet, and T. Foreword By-Haug, *The GSM system for mobile communications*: Telecom publishing, 1992.
- [28] P. Kinney, "Zigbee technology: Wireless control that simply works," in *Communications design conference*, 2003, pp. 1-7.
- [29] J. Cai and D. J. Goodman, "General packet radio service in GSM," *IEEE Communications Magazine*, vol. 35, pp. 122-131, 1997.
- [30] Y. Rodriguez and B. Garcia, "Programmable multi-function z-wave adapter for z-wave wireless networks," ed: Google Patents, 2012.
- [31] E. Avakian, "Infrared data communication system," ed: Google Patents, 1988.
- [32] W.-F. Alliance, "Wi-Fi Protected Access: Strong, standards-based, interoperable security for today's Wi-Fi networks," *White paper, University of Cape Town*, pp. 492-495, 2003.
- [33] G. A. Covic and J. T. Boys, "Inductive power transfer," *Proceedings of the IEEE*, vol. 101, pp. 1276-1289, 2013.
- [34] h. w. l. c. Labcenter Electronics Corporation, "Proteus ISIS Professional," ed, 1989-2015.
- [35] W. Klieber, L. Flynn, A. Bhosale, L. Jia, and L. Bauer, "Android taint flow analysis for app sets," in *Proceedings of the 3rd ACM SIGPLAN International Workshop on the State of the Art in Java Program Analysis*, 2014, pp. 1-6.
- [36] A. Martinaitis and K. Daunoraviciene, "Low cost self-made pressure distribution sensors for ergonomic chair: Are they suitable for posture monitoring?," *Technology and Health Care*, pp. 1-9, 2018.